Antibody Functionalization onto Microraft Arrays for Nonadherent Cell Capture and Sorting

By

Saurin Kantesaria

Senior Honors Thesis

Department of Biomedical and Health Sciences Engineering

University of North Carolina at Chapel Hill

3/31/2018

Approved:

_____

Dr. Nancy Allbritton, Thesis Advisor

Dr. Angela Proctor, Committee Member

Dr. Devin Hubbard, Committee Member

Acknowledgements:

I would like to thank Nancy Allbritton, Angela Proctor, and Devin Hubbard for being on my thesis committee and helping draft this thesis as well as Matthew DiSalvo and Yuli Wang for helping to guide me through the whole process. I would also like to thank the Allbritton lab as a whole for making this work possible.

Section 3: Table of Contents

Section 4: Abstract

Microraft arrays are cell-sorting devices the Allbritton lab has developed; they consist of a grid of thousands of transparent, magnetic cell carriers or "microrafts" embedded in a polymer membrane. Cells can be cultured on these devices and microrafts with cells can be dislodged from below using a microneedle. The dislodged microrafts can be magnetically manipulated for various downstream biological applications and bioassays. While microraft arrays can easily sort adherent cell lines such as cancer and stem cells, many highly desirable samples for cell sorting applications include nonadherent cells such as lymphocytes and other blood cells. These cell types do not attach to microrafts during culture and cannot be sorted efficiently or accurately with the current microraft platform. To enable flexible nonadherent cell sorting capable of complex phenotypic sorting criteria, a nonadherent cell capture method was investigated by attaching cell-specific antibodies onto microrafts to adhere cells to the surface. Methods of antibody attachment, such as adsorption and covalent attachment of recombinant Protein A/G (Pr A/G) and biotin amplification on microrafts were compared using fluorescence intensity readings after attachment of fluorophore-conjugated antibody to modified surfaces. It was found that adsorption of Pr A/G yields the highest and most consistent fluorescence intensity outputs. A preliminary sorting experiment comparing the sorting efficiency of Kasumi-3 ($CD34^+$) and K562 ($CD34^-$) cells on microrafts with anti-CD34 attached to Pr A/G-treated microrafts and plain, plasma-treated microrafts showed high cell sorting efficiencies (13.0% Kasumi-3 cells sorted, Control; 57.1% Kasumi-3 cells sorted, Pr A/G) and high sorting specificity (0.0% K562 cells sorted, Pr A/G; 57.1% Kasumi-3 cells sorted, Pr A/G) with this method.

Section 5: Introduction

Microraft arrays are cell-sorting devices that rely on a polydimethylsiloxane (PDMS) membrane to function. The microarrays contain a 1 square inch grid of thousands of transparent, magnetic cell carriers, or "microrafts", embedded in a PDMS membrane bound to a plastic cassette by PDMS glue (**Fig. 1**). Microrafts with adhered cells are dislodged from below using a microneedle[1-2] and can be magnetically manipulated and used for downstream applications such as PCR.

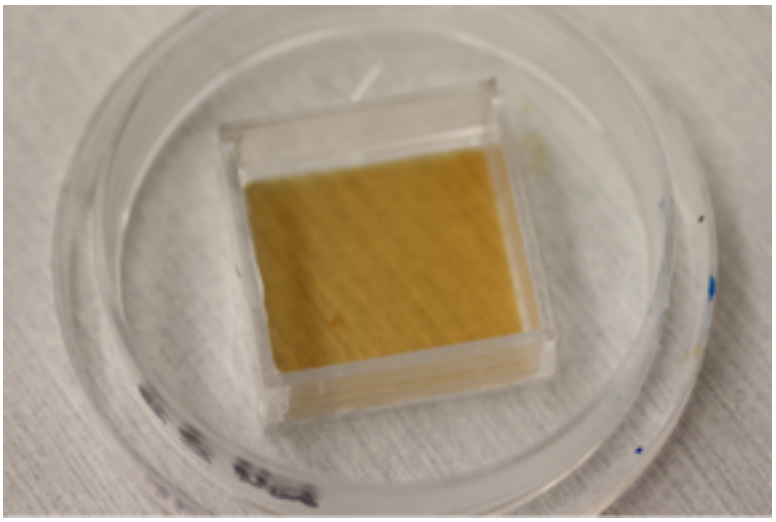

Fig. 1 *Complete microraft array attached to a cassette.*

While microraft arrays can easily sort adherent cell lines, such as cancer and stem cells, many highly desirable samples for cell sorting applications include nonadherant cells such as lymphocytes, which do not attach to microrafts during culture and cannot be sorted efficiently or accurately using this method. Furthermore, applications involving complex primary samples, such as sorting circulating tumor cells (CTCs) from blood, require pre-screening and filtration methods to perform a sort to enrich samples containing rare cell types. Samples with different cell types would otherwise require multiple sorts to purify the sample to a particular cell type, whereas samples with many cells would require filtration to even view cells of interest.

Previously reported methods for capture and sorting of nonadherent cell types utilize antibodies[3], aptamers[4], and physical[5] properties of cells such as fluorescence activated cell sorting (FACS) and inertial microfluidic sorters, but these methods each have

limitations. FACS, for example, requires expensive and bulky instrumentation, is prone to contamination, and has substantial impact on cell viability[6]. Inertial microfluidic sorting, as another example, can only sort dilute cells by limited criteria such as size and density[7].

To overcome these limitations, the Allbritton lab developed a method termed gelatin-encapsulation to sort nonadherent cells using microraft arrays[8]. Attayek *et al.* cultured nonadherent cells within cup-shaped microrafts that restricted their movement. Once cells of interest were identified, the entire microraft array was encased in 4°C gelatin to isolate nonadherent cells and keep them associated with a specific microraft; this allowed microrafts and their associated nonadherent cells to be released and collected with minimal cell loss or damage. The sorted and encapsulated cells were released from the gelatin by melting the hydrogel at 37°C. While gelatin encapsulation was shown to have 100% cell sorting efficiency, the method has distinct limitations preventing it from being useful for all cell types and experiments. The requirement for temperature cycling from 4°C to 37°C can negatively impact the viability of cells. Furthermore, the scale of cell sorting is limited using gelatin encapsulation, since the cell sorting is performed at 37°C, but the gelatin must remain cool during the sorting process. Lastly, the gelatin hydrogel may be an undesirable alteration to the cell culture environment for some cells, although it is only present for a short period. An alternate method for sorting nonadherant cells would extend the ability of microrafts to sort nonadherant cells. Here I have developed the initial basis for a nonadherant cell capture method by functionalizing cell-specific antibodies onto polystyrene (PS) microrafts.

Antibody or protein functionalization to polystyrene is a commonly used technique to capture cells[6-7][9-13]; however, optimization of the antibody density on the array was

needed to ensure a high cell capture and transfer efficiency. Different functionalization methods include simple adsorption of recombinant Protein A/G (Pr A/G)[14][11]; covalent modification with plasma treatment, 3-aminopropyltriethoxysilane (APTES) and succinic anhydride to introduce carboxyl moieties onto the surface for EDC/NHS covalent linkage to proteins[9][12]; and alternating biotin/streptavidin to increase the number of binding sites for a biotinylated target (biotin amplification)[13][15]. Ideally, covalent modification will lead to more Pr A/G being permanently bound to the microrafts, preventing more protein from being washed off. Furthermore, biotin amplification should also create significantly more sites for biotinylated antibody to bind to than Pr A/G alone. It was thus expected that the ideal surface modifications would be biotin amplification followed by covalent modification and finally adsorption.

Section 6: Methods and Materials

6.1: Preliminary Cell Sorting and Fluorescence Quantification

One test array coated with Pr A/G (Pierce Thermo Scientific) followed by antibody, and one control array (plasma treatment only), were fabricated as stated previously[1] followed by plasma treatment for 2 min to modify the surface to be more hydrophilic. Arrays were left exposed to air for a minimum of 2 days to allow for PDMS hydrophobic recovery. Polystyrene remains hydrophilic for months after plasma treatment whereas PDMS does so only for ~2 days[16]. This step is necessary to minimize nonspecific adsorption of Pr A/G or antibodies to the PDMS. Arrays were imaged for background green fluorescence using a FITC filter during this step and were sterilized for 30 min in EtOH in a culture hood.

Arrays were washed 3X for 5 min with phosphate buffered saline (PBS; 137 mM NaCl, 2.7 mM KCl, 10mM NaH_2PO_4, 1.75mM KH_2PO_4, pH 7.4) and Pr A/G (500 µL, 10 µg/mL in PBS) was applied to the test array overnight at 4°C. The test array was washed with PBS as before and the array was incubated overnight at 4°C with 10 µg/mL anti-human CD44 FITC-conjugated antibody (BD Biosciences) in PBS. The test array was washed with PBS and green fluorescence was quantified utilizing epifluorescence microscope images to integrate fluorescence over an area of four 2237 µm by 1671 µm field of views (FOVs).

K562 cells were cultured one week in advance and an aliquot of ~0.5 cells/microraft was stained with Hoechst (1:1000 dilution) in PBS at 37°C for 30 min to label cell nuclei. These cells were loaded onto the arrays, centrifuged (500 rcf, 3 min), and incubated at 37°C for 1 hr for cell binding to antibodies. Arrays were washed with PBS and imaged with an inverted epifluorescence microscope (Nikon Eclipse TE2000-U) with a DAPI filterset to

locate cell nuclei in the same 4 FOVs. Cell counts before and after array washing were quantified from fluorescence microscopy images using a custom MATLAB script, which extracted cell counts by manual intensity thresholding of the Hoechst fluorescence images and counting the number of connected components. Cell transfer efficiency was calculated by identifying microrafts with single cells and releasing, collecting, and transferring them to individual wells of a 96-well plate.

All fluorescence images requiring quantification were performed with a fluorescent bead calibration prior to each imaging session. A custom MATLAB script was written to extract the average microraft fluorescence intensities with standard deviations for coated and control conditions, dividing all pixel intensities by the average pixel intensities of the bead images.

6.2: Fluorescence Quantification of Adsorption versus Covalent Modification

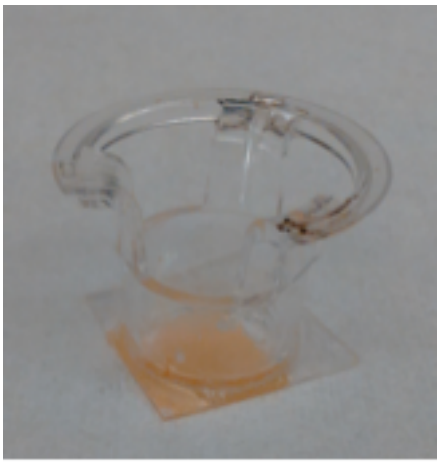

Fig. 2 *Completed Transwell array glued with PDMS to a quarter of the original array.*

To maximize the yield of samples per glass-backed array, arrays were cut into fourths and glued to Transwells (Corning). The bottom membranes of commercial Transwells were removed with tweezers and excess adhesive was scraped off with a razor blade and sandpaper. The Transwells were rinsed with ethanol (EtOH), dried, and glued to each quarter of an array with 10:1 PDMS:crosslinker. This was cured for 20 min at 70^{o}C

and carefully removed from the glass via razor blade (**Fig. 2**). A single array yields one experimental replicate for both experimental conditions (adsorption and covalent) and their respective controls.

The overall experimental setup compares adsorption and covalent modification amongst each other and to nonspecific adsorption controls for each method as shown (**Fig. 3**).

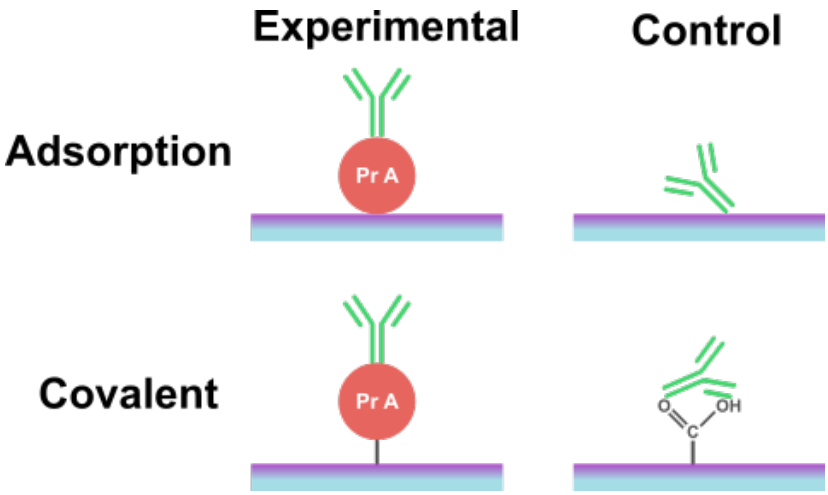

Fig. 3 *Visual representation of experimental and control conditions comparing adsorption and covalent attachment of Pr A/G.*

Adsorption of Pr A/G onto arrays was accomplished as stated above; however, each Transwell was incubated with 10 µg/mL Pr A/G solution overnight at 4°C, washed with PBS 3x, then incubated with 10 µg/mL AlexaFluor-647 IgG antibody solution for 1 hr at 25 °C, and washed 3x with PBS.

The antibody was changed to a generic IgG functionalized with AlexaFluor-647 due to lower background of the microrafts in the far-red region. The control for this condition involved applying plasma treatment as described above, and directly depositing the antibody solution after array sterilization.

Covalent modification was performed by plasma treatment as previously stated, followed by applying a monolayer of APTES (3-aminopropyltriethoxysilane) to the microrafts via deposition of 100 µL of 98.0% APTES solution in a vacuum chamber overnight. The array was washed 3x with DI water (1 min per wash) to remove excess

silane and immersed in succinic anhydride (10 mM in EtOH) overnight at 25 °C. The array was glued to the Transwell insert with PDMS, and sterilized as described above. An EDC/NHS reaction was performed to covalently link the carboxyl moieties on the Transwell array to the amine groups on Pr A/G. The Transwell array was incubated an EDC/NHS solution (60 mM EDC, 15 mM NHS, in MES buffer 0.1 M pH 5, 1:1:1 ratio) for 1 hr at 25 °C and washed 3x with PBS (2 min per wash) to remove excess solution. Pr A/G and the antibody were added in succession as previously stated. The control for this condition lacked both the EDC/NHS reaction and incubation with Pr A/G, and antibody was plated onto the Transwell array directly after sterilization and succinic anhydride modification. All four conditions were performed in triplicate on separate Transwell arrays.

A modified version of the abovementioned MATLAB script was used to quantify mean fluorescence intensities at the centers of microrafts in a more precise and consistent fashion along the entire array. Background subtraction was performed by subtracting the mean fluorescence intensities of the same microraft array before applying antibody from these raw fluorescence intensities under the same fluorescence channel. An

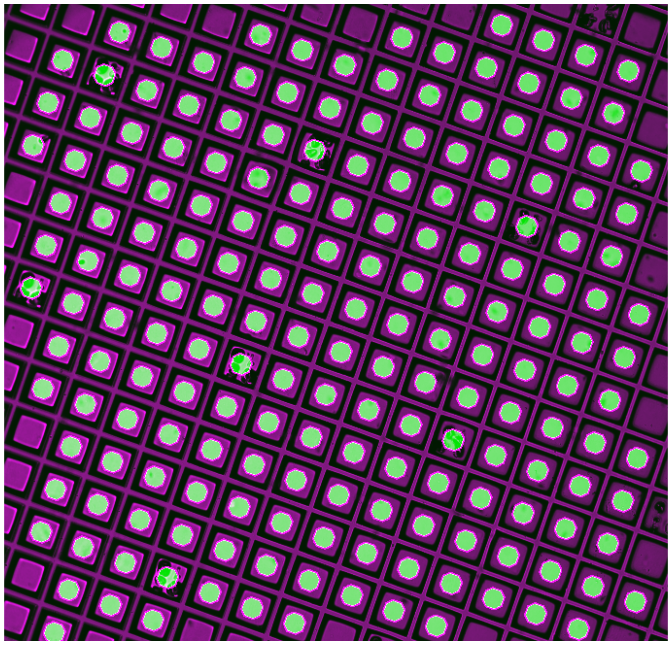

Fig. 4 *Representative image of MATLAB script identifying microraft centers in brightfield to sample fluorescence intensities in these regions in Cy5 channel.*

example of the image segmentation regions taken per FOV is shown in **Fig. 4**. A two-way ANOVA and multiple comparison test was used to test for differences between experimental and control conditions.

6.3: Adsorption versus Biotin Amplification Fluorescence Quantification

Pr A/G modification was performed as described above with the same nonspecific adsorption control. The antibody was exchanged for one that matched the fluorophore in the biotin amplification condition (Atto-594 IgG, Millipore Sigma).

For the biotin amplification condition, the array was plasma treated and sterilized as described above. An EDC/NHS reaction was performed to better link the streptavidin to the plasma treated polystyrene surface of the microrafts. For each cycle thereafter, 7.5 μg/mL of streptavidin solution (Millipore Sigma) was added to the Transwell array, followed by a 1x PBS wash. 1.5 μg/mL biotinylated bovine serum albumin (biotin-BSA) solution (Millipore Sigma) was added, followed by another PBS wash. All wash steps and solution steps were performed in immediate succession. A total of 20 cycles per replicate was used as the optimal number based on previous results[15]. On the 20th cycle, a 0.057 μM Atto 594-biotin solution was added instead of a fluorescent antibody at the same molar concentration as the antibody in the Pr A/G condition. The array was incubated overnight at 4^{o}C and washed 3x with PBS (5 min per wash). All four conditions were performed in triplicate on separate Transwell arrays and the fluorescence intensities for each Transwell array were quantified using the same MATLAB script as before. A two-way ANOVA and multiple comparison test was used to test for differences between experimental and control conditions.

6.4: Preliminary Cell Sorting with K562 and Kasumi-3 Cell lines

One replicate of a cell sorting experiment comparing transfer efficiencies of K562 and Kasumi-3 cells of the adsorption condition and a non-coated control was performed. Raft arrays divided into four chambers were used for this experiment. For the adsorption condition, Pr A/G and anti-human anti-CD34 antibody (Santa Cruz Biotechnology) were adsorbed to a microraft array as before. Anti-CD34 was chosen due to its specificity for Kasumi-3 cells over K562 cells[17][18]. A negative control microraft array was plasma treated as before and not coated with antibody.

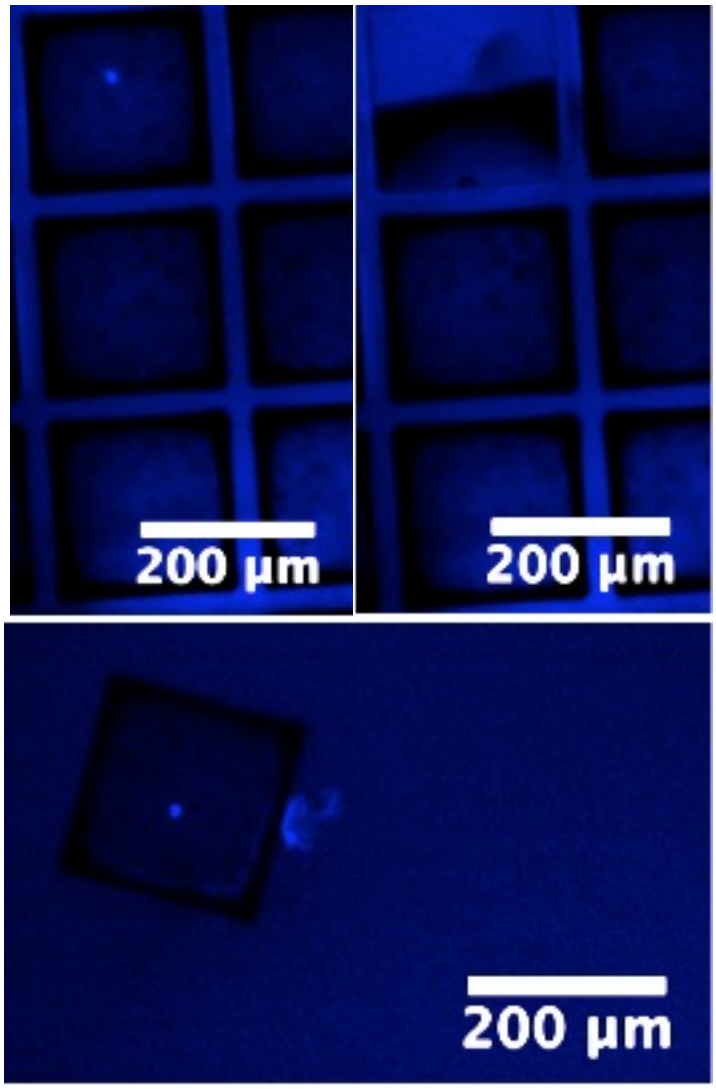

Fig. 5 *Representative image of cell transfer process for testing sorting efficiencies of K562 and Kasumi-3 cells (10x, 1392x1040 pixels, DAPI). Cells are first identified by size (top left), released (top right), then transferred over via magnetic wand to a 96-well plate (bottom).*

Two cell lines, one CD34 positive (Kasumi-3) and one CD34 negative (K562), were plated at 1000 cells/mL (~0.5 cells/microraft) to maximize the number of microrafts with single cells. Initially, K562s were stained with Hoechst (1:1000 dilution) at 37°C for 30 min in a separate conical tube from Kasumi-3s, which were stained with Draq5 (1:5000 dilution) at 37°C for 30 min. For each tube, excess media was removed and replaced, and

both cell solutions were combined into a single mixture. However, during the extended imaging time, both cell types eventually were stained with both Draq5 and Hoechst. Thus, the staining was performed again on the microarrays using Hoechst alone at higher concentrations for ease of identifying cells from background, and the significant size differences (4 μm diameter of Kasumi-3 *versus* 20 μm diameter of K562) between the two cell lines were used to distinguish the cell type. Cells were imaged throughout the release process (DAPI) as shown (**Fig. 5**). Transfers were performed as before with a 96-well plate containing conditioned and fresh media (25:75 ratio by volume)[1-2]. Microrafts containing either or both cells were released and transferred to the 96-well plate in total. The number of Kasumi-3s and K562s before release and after transfer was quantified manually after imaging and cell type was differentiated by size.

Section 7: Results

7.1: Preliminary Cell Sorting and Fluorescence Quantification

Preliminary experiments tested extent of antibody attachment, cell capture efficiency, and cell transfer efficiency of antibodies bound to Pr A/G adsorbed to the microraft surface. As stated previously, this was performed by comparing the mean fluorescence intensities at the centers of microrafts produced by fluorescent antibodies attached to either Pr A/G or a plasma-treated surface. Corrected fluorescence intensities for microrafts in green fluorescence were calculated by dividing pixel intensities by average calibration bead intensities. This was quantified for uncoated microrafts and microrafts coated with FITC-conjugated CD44 as shown (**Fig. 6**). An unpaired t-test (alpha = 0.05) between these values showed a statistically significant difference between the two conditions.

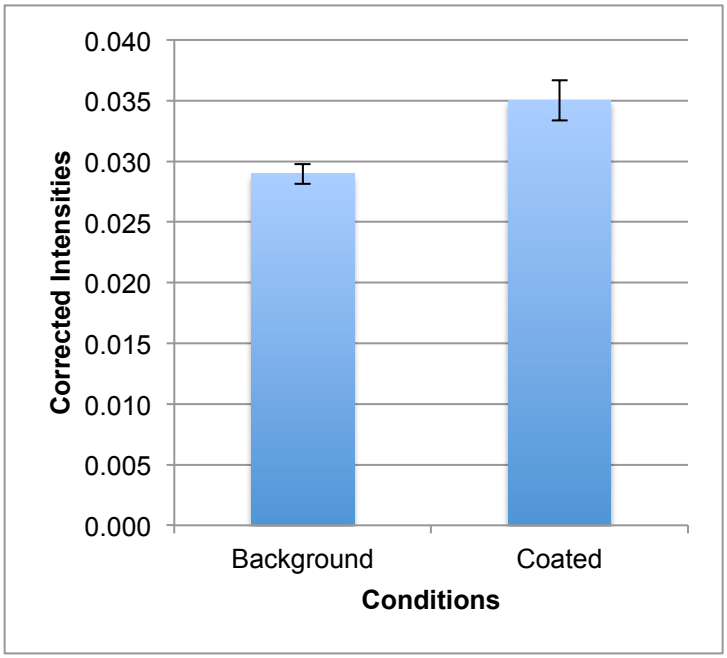

Fig. 6 *Corrected FITC fluorescence intensities (raw intensities divided by average bead intensities) for uncoated (N=1) (background) and Pr A/G and antibody-coated microrafts (N=4).*

Cell capture efficiencies for the negative control and antibody-coated array with Pr A/G were 18.9% (7/37) and 82.6% (114/138), respectively (**Fig. 7**). Cell transfer efficiency for the antibody-coated array with Pr A/G was 33.3% (9/27).

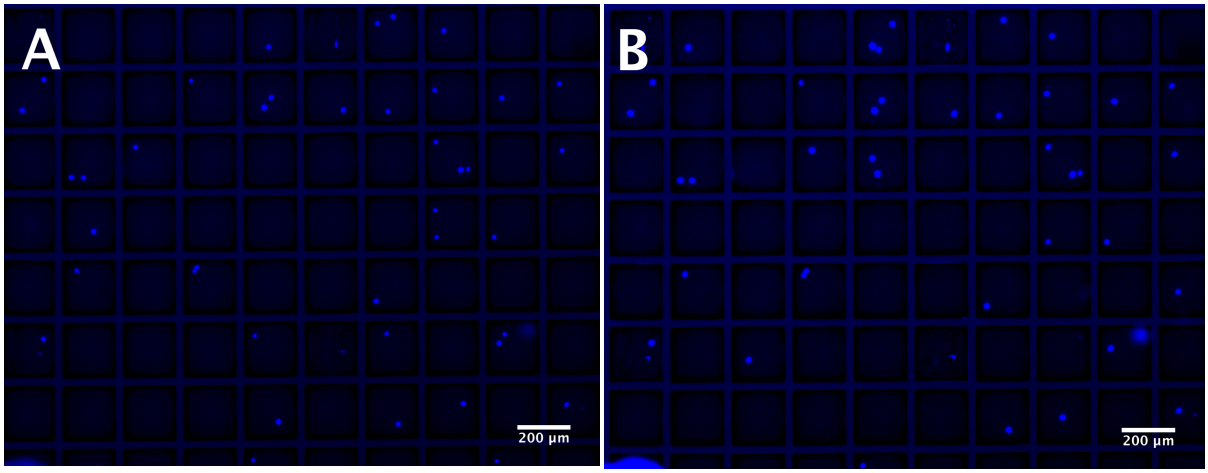

Fig. 7 *Representative fluorescence microscopy images (4x, 1392x1040 pixels, DAPI) of Hoechst nuclear stain of K562 cells bound by CD44 antibody to microraft arrays by Protein A/G (A) before and (B) after washing with PBS.*

7.2: Adsorption versus Covalent Modification Fluorescence Quantification

Covalent attachment of Pr A/G to the surface of the polystyrene microrafts was investigated and the relative amount of antibody bound to the surface was compared to that of Pr A/G attached to the surface of microrafts through adsorption alone. Mean background corrected fluorescence intensities for each condition across all replicate means were: Adsorption (4884.0 ± 1554.2), Covalent (1048.9 ± 202.2), Adsorption Control (175.2 ± 233.8), Covalent Control (176.2 ± 216.0). As shown by both the graph (**Fig. 8**) of mean fluorescence intensities from the microraft centers and a 2-way

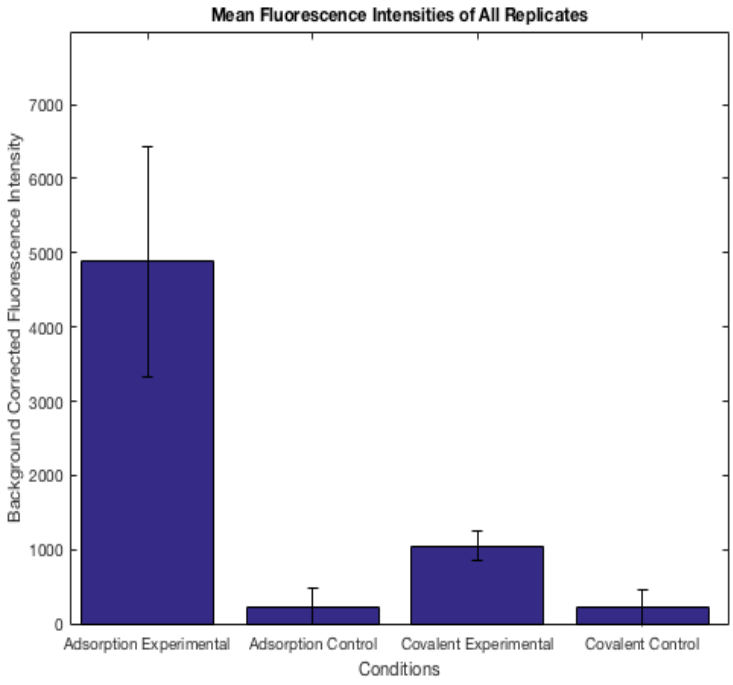

Fig. 8 *Mean background corrected fluorescence intensities at microraft centers gathered using MATLAB script for each condition (covalent modification versus adsorption) in triplicate.*

ANOVA and multiple comparison test, the mean fluorescence intensities of the adsorption experimental condition significantly differed from both those of the nonspecific adsorption control and the covalent modification experimental condition ($p<0.05$, Control vs Experimental Row p-value: 0.0013, Experimental vs Experimental Column p-value: 0.0094). The mean fluorescence intensities for the covalent modification experimental condition also significantly differed from those of its control as well.

Examining the distributions of fluorescence intensities for both experimental conditions (adsorption and covalent), the shapes of the histograms and ranges are fairly consistent for both distributions as well (**Fig. 9**).

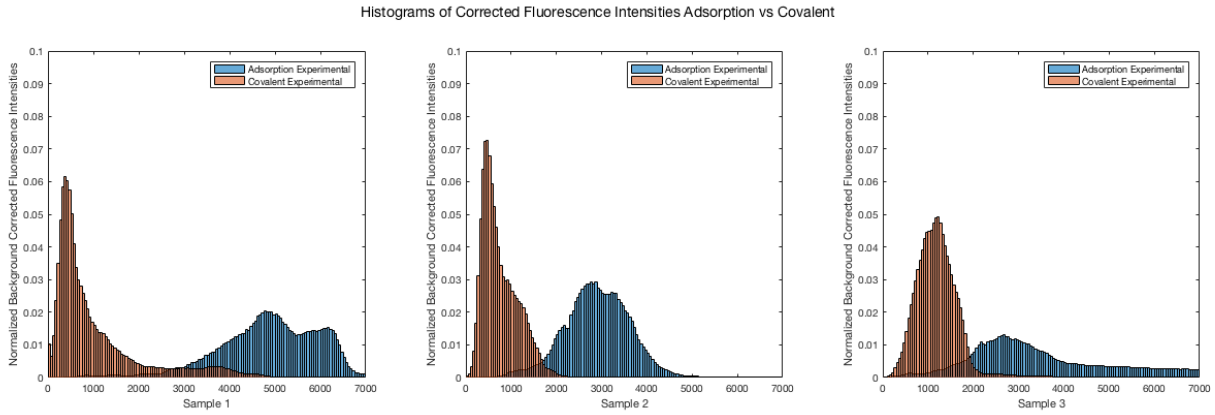

Fig. 9 *Histograms showing normalized background corrected fluorescence intensity distributions of adsorption (blue) and covalent (orange) experimental conditions per replicate.*

Qualitatively examining the spatial distribution of antibody fluorescence for both experimental conditions, the adsorption experimental condition had an even and fairly consistent distribution whereas that for the covalent experimental condition was noticeably uneven (**Fig. 10**).

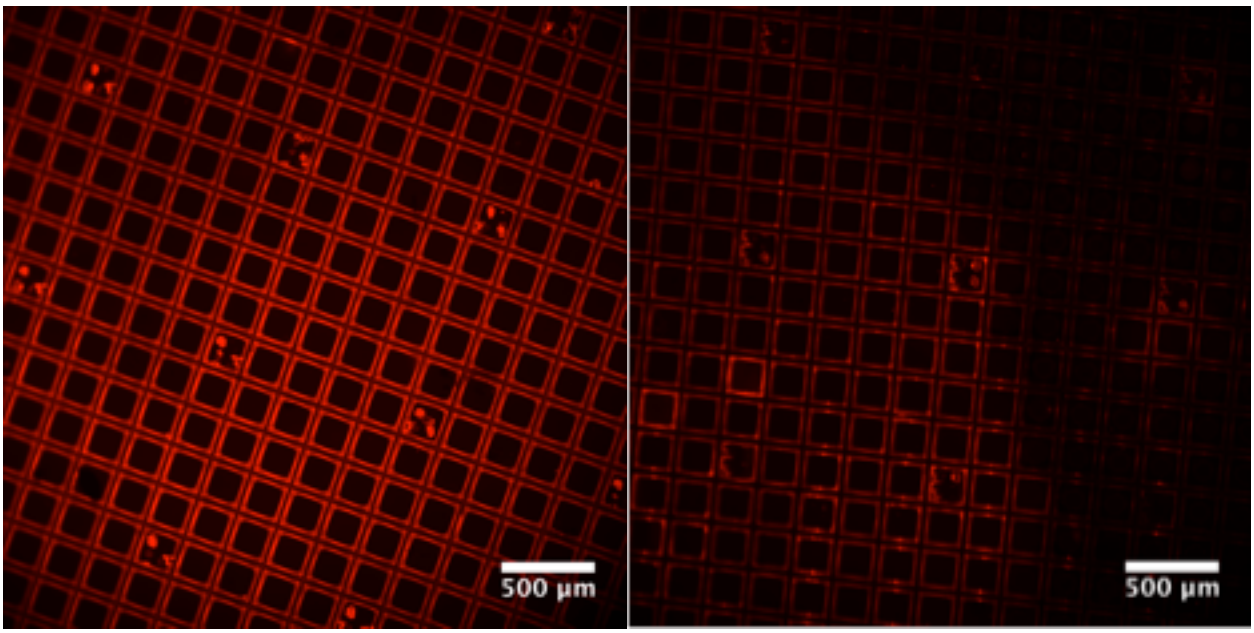

Fig. 10 *Representative fluorescence microscopy images (4x, 1392x1040 pixels, Cy5) of (fluorophore)-IgG attached to Pr A/G in the adsorption condition (left) and covalent condition (right) on Transwell arrays.*

7.3: Fluorescence Quantification of *Adsorption versus Biotin Amplification*

After determining that adsorption yielded higher fluorescence intensities on average than covalent modification, the adsorption condition was compared with a slightly modified version of the biotin amplification protocol from Chu *et al.* on Transwell arrays[15].

Mean background corrected fluorescence intensities for each condition across all replicate means were: Amplification (1617.5 ± 729.9), Amplification Control (4616.1 ± 714.1), Adsorption (4051.0 ± 4154.5), Adsorption Control (3380.5 ± 2010.3) (**Fig. 11**). When comparing the 20 cycles of biotin amplification to adsorption of Pr A/G to microrafts, a 2-way ANOVA and multiple comparison test found no significant differences between controls and experimental conditions as well as experimental conditions in terms of mean background corrected fluorescence intensities at the centers of microrafts ($p>0.05$, Control vs Experimental Row p-value: 0.4184, Experimental vs Experimental Column p-value: 0.6723).

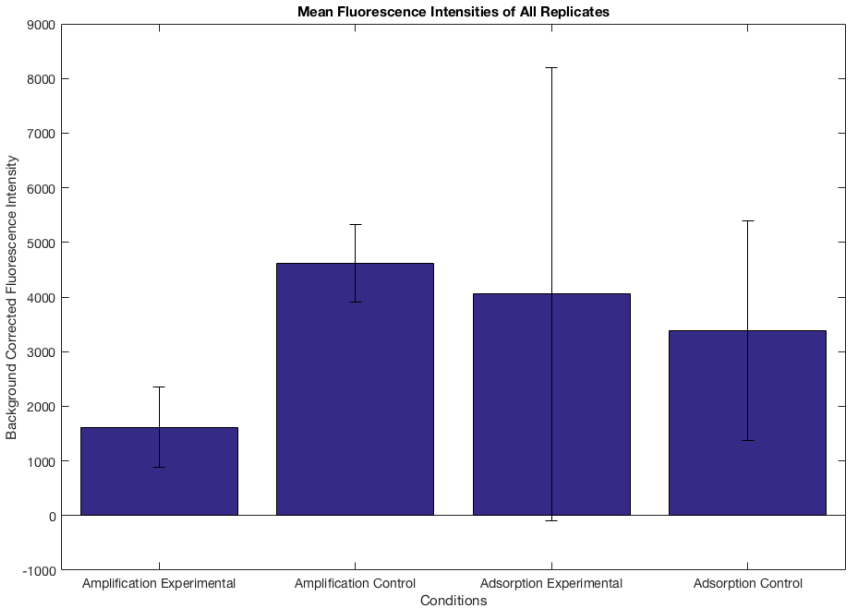

Fig. 11 *Mean background corrected fluorescence intensities at microraft centers gathered using MATLAB script for each condition (amplification versus adsorption) in triplicate.*

Examining the normalized background corrected distributions of each replicate, however, adsorption of Pr A/G to microrafts qualitatively had overall higher fluorescence values than those for biotin amplification (**Fig. 12**).

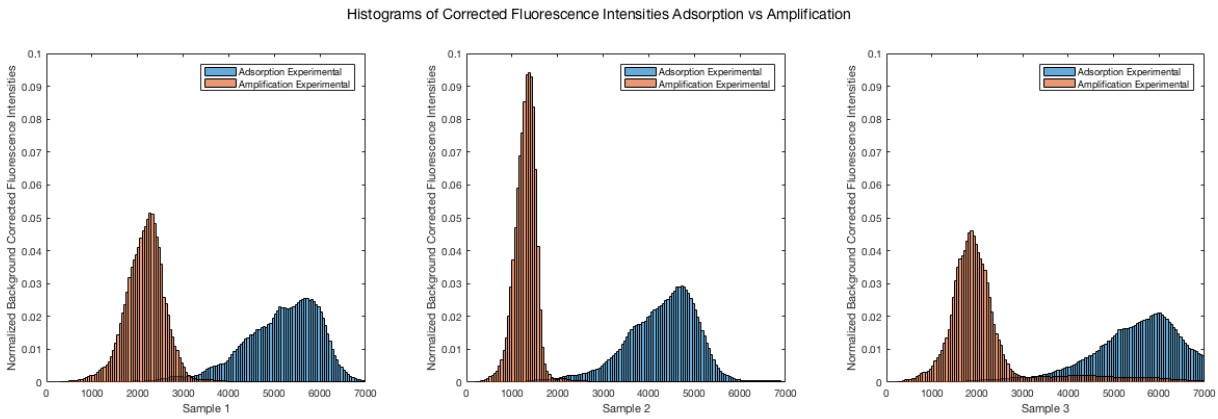

Fig. 13 *Histograms showing normalized background corrected fluorescence intensity distributions of adsorption (blue) and 20 cycles of biotin amplification (orange) experimental conditions per replicate.*

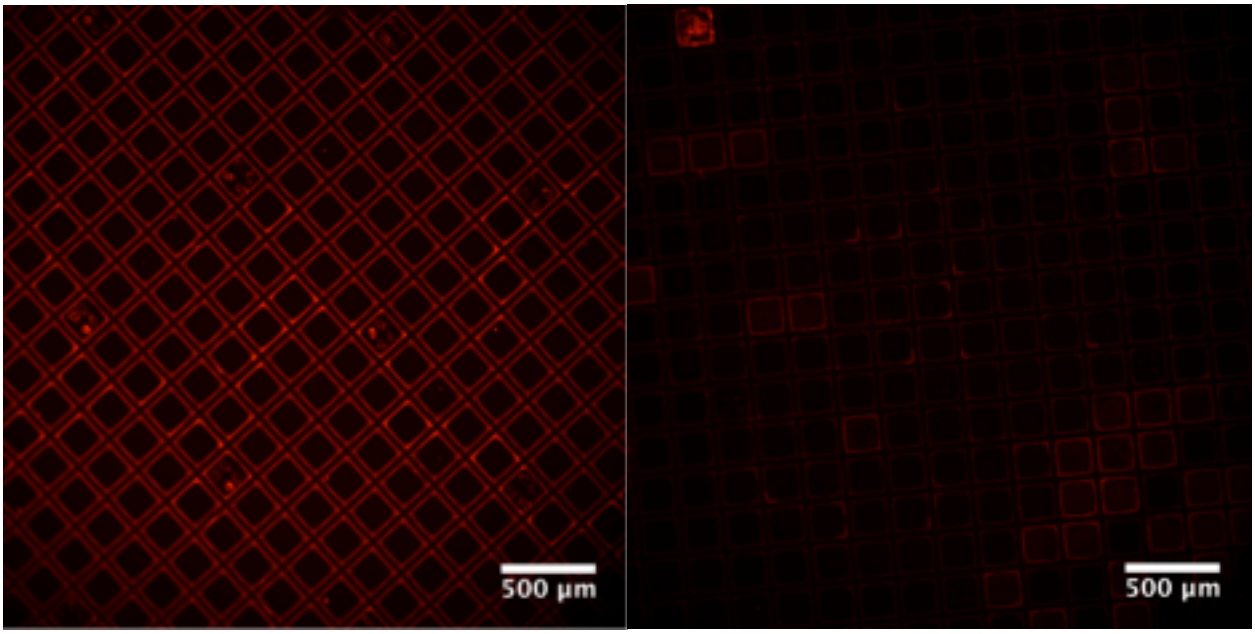

Fig. 12 *Representative fluorescence microscopy images (4x, 1392x1040 pixels, Cy5) of (fluorophore)-IgG attached to Pr A/G in the adsorption condition (left) and 20 cycles of biotin amplification condition (right) on Transwell arrays.*

Qualitatively examining the spatial distribution of fluorescence for both experimental conditions, the adsorption condition again had an even and fairly consistent distribution whereas that for the amplification condition was primarily uneven (**Fig. 13**)

7.4: Cell Sorting with K562 and Kasumi-3 Cell lines

Preliminary sorting efficiencies for sorting Kasumi-3 cells from K562 cells with the Pr A/G adsorption method, which based on previous results was found to yield the highest and most consistent fluorescence intensities, were obtained on a single replicate of conditions with K562 and Kasumi-3 cell lines plated on the same array. Anti-CD34 was used as the antibody to sort for Kasumi-3 cells as described in the methods section. Sorting efficiencies were determined by comparing cells present before release on the array to how many were present after transfer to a 96-well plate (**Table 1**).

Condition	**K562 Sorting Efficiency (after release/before release)**	**Kasumi-3 Sorting Efficiency (after release/before release)**
Control	16.7% (4/24)	13.0% (3/23)
Pr A/G Adsorption	0.0% (0/16)	57.1% (12/21)

Table 1. *Preliminary sorting efficiencies comparing sorting of K562 and Kasumi-3 cell lines on a non-coated, plasma-treated control array to a plasma-treated array with Pr A/G adsorbed to the surface and anti-CD34 attached to Pr A/G. Percentages of sorting efficiency are expressed as cells successfully transferred to cells present before transfer.*

Section 8: Discussion and Conclusion

Through initial cell sorting experiments comparing adsorption of Pr A/G and anti-CD44 to microraft arrays to a plain plasma-treated microraft array, it was found that Pr A/G adsorption to the microraft surface coupled with antibody attachment increased nonadherent cell capture efficiency; however, the transfer efficiency could still be significantly improved. This lower than expected efficiency could have been a result of low antibody-antigen binding strength and low numbers of CD44 on K562 cell surfaces. Another explanation could be the potentially high shear forces exerted on microrafts when being transferred out of the microraft array media and onto the 96-well plate. These forces could potentially be strong enough to shear cells off the microraft. Pr A/G already orients antibodies along the Fc domain such that the antigen binding site should always be exposed; however, many antibodies bound to the surface that bind to a given antigen could also sterically hinder other antibodies attempting to bind to the same antigen. Some other factors that may have affected fluorescence data include high autofluorescence levels of the microrafts in the FITC channel and perhaps low levels of antibody on the microraft surfaces. Based on this, for future experiments, it was noted that an antibody with higher abundance on cell surfaces and potentially stronger binding interactions would be needed. In addition to this, other methods of antibody attachment that would potentially increase the number of attachment sites were investigated, including covalent attachment of Pr A/G to microraft surfaces as well as biotin amplification.

Fluorescence intensity readings of fluorophore-conjugated antibodies were used to compare the relative amounts of antibody attached to the surfaces of microrafts for all methods. The method producing the highest and most consistent fluorescence intensities

was chosen when comparing any two methods and this condition was compared against each successive method to be tested.

Comparing adsorption of Pr A/G to covalent attachment of Pr A/G to microraft surfaces, it was found that adsorption had significantly higher and more consistent fluorescence intensities at the centers of microrafts. Originally, it was thought that covalent modification would increase the amount of Pr A/G attached to microrafts compared to adsorption since the Pr A/G would be covalently bound to the surface as opposed to being more loosely attached via adsorption. Thus, Pr A/G bound through adsorption would be more likely to be washed away. APTES and succinic anhydride ideally would create more carboxyl moieties for covalent attachment to the amine groups on Pr A/G via EDC/NHS chemistry. However, this was not the case given the current method. While some individual microrafts did indeed have higher fluorescence intensities at their centers, most did not and the coating was uneven. While the protocol was tested with various modifications, further optimization of reaction times and reagent concentrations may achieve a more consistent attachment. Future work may also investigate alternative methods of covalent modification such as: adding functional-spacer-lipid constructs such as Kode to cells to increase the types of linkers that can be used[19]; covalent linkage of DNA to cell membrane amines[20]; or covalent linkage of other peptides such as RGD sequences which bind to integrin adhesion receptors[21].

Between adsorption of Pr A/G and 20 cycles of biotin amplification, adsorption was also found to have higher and more consistent fluorescence intensities at the centers of microrafts. Biotin amplification was hypothesized to produce more attachment sites, due to the increases in signal Chu *et al.* found with their experiments. Ideally, streptavidin bound

to the surface of microrafts would have created multiple sites for attachment of biotin-BSA, which would have created more sites for streptavidin attachment to greatly increase the ultimate number of attachment sites for biotinylated antibodies. Again, this method produced some individual microrafts with much higher fluorescence intensities at their centers than those for Pr A/G; however, the majority of microrafts had lower intensities and the coating was inconsistent across the array. Furthermore, the control for biotin amplification had higher average fluorescence than the experimental condition, indicating significant nonspecific adsorption of the fluorescent biotin. Inconsistencies could have been due to multiple possibilities, including: the many washes removing loosely bound streptavidin; potentially lower concentrations of biotin used than was required; array-specific variations in surface properties; the EDC/NHS reaction potentially chemically blocking the surface to prevent adsorption of streptavidin; or high amounts of fluorescent biotin caused quenching of the fluorescence signal when amplification was present. Other methods of amplification such as one-step incubation of biotin and streptavidin together, increasing carboxyl groups for initial linkage with streptavidin such as with adsorption of dopamine to raft surfaces, and other methods will also need to be tested in the future to expand on and improve the current method.

While the preliminary multi-cell sort between K562 and Kasumi-3 cells was performed on low numbers of cells, the results suggest that Pr A/G adsorption with a more specific antibody such as anti-CD34 can specifically and fairly efficiently sort nonadherent cells from a mixed population. In this case, Kasumi-3 cells were specifically sorted for using the Pr A/G adsorption condition, where 57.1% of Kasumi-3 cells were transferred whereas 0.0% of the K562 cells could be transferred. Furthermore, comparing Kasumi-3 sorting

efficiency across control and Pr A/G adsorption conditions, the efficiency differences were high (13.0% vs 57.1% respectively), indicating that the method has a higher sorting efficiency than plain plasma-treated microraft arrays. The discrepancy between control and adsorption sorting efficiencies for K562 cells (16.7% and 0.0%, respectively) could potentially be explained by steric repulsion between the antibodies and cell surfaces in the experimental condition. The control condition is only plasma treated and thus would most likely increase cell adhesion to some extent as a result with minimal steric interactions. Further replicates with more cells will need to be obtained with this experimental design to determine if these differences are statistically significant. One limitation of this experiment was that the Hoechst stain cannot definitively differentiate Kasumi-3 cells from K562 cells. The size difference between the two cells was fairly obvious since Kasumi-3 cells are significantly smaller than K562 cells; however, if any cells at the higher end of the Kasumi-3 size range or the lower end of K562 size range were similar in size, they would not be able to be visually differentiated. Initially, the cells were stained separately with Hoechst and Draq5 (two nuclear stains), and the media was replaced, but upon extended plating of cells, both cells were stained with these markers, likely because there was either enough Hoechst or Draq5 in the remaining media to stain other cells. Furthermore, the PDMS was also stained with Draq5, further limiting the ability to specifically differentiate these cells during these initial tests. Future experiments may need to separate the two cells or find other stains to more definitively differentiate the two such as CellTracker dyes, which are not expected to leach into solution for uptake by surrounding cells.

The goals of future work will be to gather more replicates of the multiple cell sorting trials and to sort multiple cell types with nonspecific cell attachment methods using

methods such as CellTack, poly-Lysine adsorption, and an IgM antibody attachment to Pr A/G adsorbed to microraft surfaces. Nonspecific binding agents may potentially have higher binding affinity and higher numbers of attachment sites for cells, which may increase sorting efficiency; however, they would also require an initial stain of cells to differentiate cell types of interest. Once these methods have been tested as a proof-of-concept, leukemic or other nonadherent cells will be transfected with green fluorescent protein (GFP) and purified with a single-cell sort using the Pr A/G adsorption method. Time-allowing, single-cell polymerase chain reaction will then be performed to detect for GFP DNA in these cells to show this method is possible for nonadherent cells.

Overall, it was found that simple adsorption of Pr A/G to microraft surfaces with attachment of a cell-specific antibody can increase the nonadherent cell sorting efficiency of microraft arrays. This and the other methods tested were only initial additions to a "toolkit" of surface modifications to the array and there still are many other possibilities that can further increase the current sorting efficiency. Once fully optimized, this system could help drive the development of methods for studying rare nonadherent cell types and clinically monitoring disease progression and diagnosis.

Section 9: References

1. Gach, P. C., Wang, Y., Phillips, C., Sims, C. E. & Allbritton, N. L. Isolation and manipulation of living adherent cells by micromolded magnetic rafts. *Biomicrofluidics* **5,** 32002–3200212 (2011).

2. Wang, Y. *et al.* Micromolded arrays for separation of adherent cells. *Lab Chip* **10,** 2917–24 (2010).

3. Mazutis, L. *et al.* Single-cell analysis and sorting using droplet-based microfluidics. *Nat. Protoc.* **8,** 870–891 (2013).

4. Sheng, W. *et al.* Aptamer-Enabled Efficient Isolation of Cancer Cells from Whole Blood Using a Microfluidic Device. *Anal. Chem.* **84,** 4199–4206 (2012).

5. Yang, A. H. J. & Soh, H. T. Acoustophoretic sorting of viable mammalian cells in a microfluidic device. *Anal. Chem.* **84,** 10756–62 (2012).

6. Attachment of hyaluronic acid to polypropylene, polystyrene, and polytetrafluoroethylene. *Biomaterials* **21,** 31–36 (2000).

7. Kumar Dixit, C., Kumar Vashist, S. & MacCraith, B. D. Multisubstrate-compatible ELISA procedures for rapid and high-sensitivity immunoassays. *Nat. Protoc.* **6,** (2011).

8. Attayek, P. J. *et al.* Array-Based Platform To Select, Release, and Capture Epstein–Barr Virus-Infected Cells Based on Intercellular Adhesion. *Anal. Chem.* **87,** 12281–12289 (2015).

9. Welch, N. G., Scoble, J. A., Muir, B. W. & Pigram, P. J. Orientation and characterization of immobilized antibodies for improved immunoassays (Review). *Biointerphases* **12,** 02D301 (2017).

10. Comparison of two types of acoustic biosensors to detect immunoreactions: Love-wave sensor working in dynamic mode and QCM working in static mode. *Sensors Actuators B Chem.* **189,** 123–129 (2013).

11. Vashist, S. K., Dixit, C. K., MacCraith, B. D. & O'Kennedy, R. Effect of antibody immobilization strategies on the analytical performance of a surface plasmon resonance-based immunoassay. *Analyst* **136,** 4431 (2011).

12. Vashist, S. K., Lam, E., Hrapovic, S., Male, K. B. & Luong, J. H. T. Immobilization of Antibodies and Enzymes on 3-Aminopropyltriethoxysilane-Functionalized Bioanalytical Platforms for Biosensors and Diagnostics. *Chem. Rev.* **114,** 11083–11130 (2014).

13. Lucarelli, F., Marrazza, G. & Mascini, M. Dendritic-like Streptavidin/Alkaline Phosphatase Nanoarchitectures for Amplified Electrochemical Sensing of DNA Sequences. doi:10.1021/la053187m

14. Wang, Y. *et al.* Surface graft polymerization of SU - 8 for bio - MEMS applications. *J . Micromech . Microeng . J . Micromech . Microeng* **17,** 1371–1380 (2007).

15. Chu, Y. W. *et al.* Layer by layer assembly of biotinylated protein networks for signal amplification. *Chem. Commun.* **49,** 2397 (2013).

16. van Kooten, T. G., Spijker, H. T. & Busscher, H. J. Plasma-treated polystyrene surfaces: model surfaces for studying cell-biomaterial interactions. *Biomaterials* **25,** 1735–47 (2004).

17. Inoue, T., Swain, A., Nakanishi, Y. & Sugiyama, D. Multicolor analysis of cell surface marker of human leukemia cell lines using flow cytometry. *Anticancer Res.* **34,** 4539–50 (2014).

18. Atcc.org. (2018). Kasumi-3 ATCC ® CRL-2725™ Homo sapiens peripheral blood acute myeloblastic leukemia. Available at: https://www.atcc.org/en/Products/All/CRL-2725.aspx [Accessed 27 Mar. 2018].

19. Kode™ Technology - Overview. Kodecyte.com (2018). Available at http://www.kodecyte.com/tech-overview/technology-overview.html.

20. Hsiao, S. C., Shum, B. J., Onoe, H., Douglas, E. S., Gartner, Z. J., Mathies, R. A., . . . Francis, M. B. (2009). Direct Cell Surface Modification with DNA for the Capture of Primary

Cells and the Investigation of Myotube Formation on Defined Patterns. *Langmuir: the ACS journal of surfaces and colloids*, **25**(12), 6985-6991. doi:10.1021/la900150n.

21. Gabriel, M., Nazmi, K., Dahm, M., Zentner, A., Vahl, C.-F., & Strand, D. (2012). Covalent RGD Modification of the Inner Pore Surface of Polycaprolactone Scaffolds. *Journal of Biomaterials Science, Polymer Edition*, **23**(7), 941-953. doi:10.1163/092050611X566793.

22. Huang, B., Wu, H., Kim, S. & Zare, R. N. Coating of poly(dimethylsiloxane) with n-dodecyl-β-d-maltoside to minimize nonspecific protein adsorption. *Lab Chip* **5,** 1005 (2005).

23. Custódio, C. A. *et al.* Photopatterned Antibodies for Selective Cell Attachment. *Langmuir* **30,** 10066–10071 (2014).